

X-ray spectral variability of the Seyfert galaxy NGC 4593

K.K. Ghosh and S. Soundararajaperumal

Indian Institute of Astrophysics, Vainu Bappu Observatory, Kavalur, Alangayam, N.A., T.N., 635701 India

Received February 13, accepted December 16, 1992

Abstract. X-ray (0.1–10 keV) spectra of NGC 4593 were obtained with EXOSAT on seven epochs between 1984 and 1986 using the low and medium energy detectors. Detailed results of the spectral analysis of the seven spectra (obtained from the EXOSAT database) of this galaxy are presented here. Power-law, two power-law, thermal bremsstrahlung and broken power-law models with fixed absorption (fixed with the galactic column density value) were used to fit the data. Broken power-law + fixed absorption model describes the best fit to the spectra than that obtained from other models. However this model cannot completely fit the soft excess emission present in the spectra of NGC 4593, which leads to the suggestion that, most probably, two soft emission components are present in this galaxy. A highly significant ($>99.9\%$) emission line feature was detected which could be the redshifted 6.4 keV fluorescent Fe-K line. Detected soft excess variability and the Fe-K emission line is reported here for the first time for NGC 4593. The significance of these results is discussed.

Key words: active galactic nuclei – galaxies: NGC 4593 – galaxies: Seyfert – X-ray spectrum

1. Introduction

NGC 4593 is a bright ($V=13.15$, $B-V=0.8$, $U-B=-0.19$ and absolute magnitude is -20.5 ; Véron et al. 1982; Véron & Véron 1986), nearby ($z=0.009$; Mac-Alpine et al. 1979) Seyfert 1 galaxy (Simkin et al. 1980) with strong broad allowed, and narrow forbidden optical emission lines (MacAlpine et al. 1979) and with weak radio emission (Ulvestad & Wilson 1984). This galaxy was first observed in the X-ray spectral region with Uhuru satellite and it was proposed that the X-ray source 4U 1240–05 is associated with the cluster Abell 1588 (Forman et al. 1978; Mitchell et al. 1979). Later on HEAO-1 observations with small error box, have identified this X-ray source (H 1238–049) with the Seyfert galaxy NGC 4593 (Marshall et al. 1978; Wood et al. 1984). Ariel V (Bell Burnell & Culhane 1979; Hayes et

al. 1981) and Einstein SSS + MPC (Holt et al. 1989) results have displayed different results about this galaxy (spectral index, $\alpha [=(\Gamma - 1)$ where Γ is the photon index] = 1 and the low energy absorption column density $N_{\text{H}} \sim 4 \cdot 10^{22} \text{ cm}^{-2}$ were obtained from Ariel V observations and Einstein results show $\alpha = 0.12 \pm 0.28$ and $N_{\text{H}} \sim 0 < 3.2 \cdot 10^{21} \text{ cm}^{-2}$). EXOSAT observed this galaxy on seven epochs between 1984 and 1986. Only one EXOSAT spectrum has been analysed by Turner & Pounds (1989) and Barr et al. (1987) and Grandi et al. (1992) have studied the flux variability of this source. A soft excess component of NGC 4593 was assessed by Turner & Pounds (1989) by fixing N_{H} at the galactic value. However no information is available about the soft excess variability of this galaxy. Also it is not known whether iron emission line is present in the spectrum of this source or not. Thus the detailed spectral analysis of this galaxy, which is not a well studied source, may provide many interesting results (soft excess variability, iron emission line, etc.). In this paper we present the results of the analysis of the seven X-ray (0.1–10 keV) spectra of NGC 4593 which were obtained from EXOSAT database (White & Giommi 1991).

2. Observations

The soft X-ray (0.1–2 keV) observations of NGC 4593 were carried out with EXOSAT on seven epochs between 1984 and 1986 using the Low Energy (LE) telescope with a Channel Multiplier Array (CMA) as the detector. Lexan 3000 (LX3), Aluminium/Parylene (Al/P) and Boron (B) filters (White & Peacock 1988) were used with the CMA detectors (de Korte et al. 1981) to obtain the spectrum of this source in the 0.1–2 keV range. Background subtracted LE count rates with errors were obtained from the EXOSAT database (White & Giommi 1991) and they were converted into the LE pulse height (PHA) spectra using the X-ray analysis and data utilization (XANADU) software package.

Hard X-ray (2–10 keV) spectra of NGC 4593 were obtained with the Medium Energy (ME) detectors (Turner et al. 1981). Eight ME detectors were divided into two halves (detectors 1, 2, 3 and 4 are collectively known as Half 1 and 5, 6, 7 and 8 as Half 2) which can be either

Send offprint requests to: K.K. Ghosh

Table 1. Log of observation of the LE and ME spectra and count rates of NGC 4593

Start time ^a	End time ^b	LE count rate ($10^{-3} \text{ cm}^{-2} \text{ s}^{-1}$)			ME count rate ^c ($10^{-3} \text{ cm}^{-2} \text{ s}^{-1}$)
		(LX3)	(A1/P)	(B)	
1984, 154, 06:30	154, 12:20	2.22 ± 0.13	1.02 ± 0.09	0.16 ± 0.02	3.45 ± 0.05
1984, 183, 00:55	183, 06:37	2.15 ± 0.15	0.95 ± 0.06	0.14 ± 0.01	4.20 ± 0.05
1985, 176, 06:05	176, 14:30	0.43 ± 0.03	0.21 ± 0.02		1.36 ± 0.04
1985, 180, 17:25	180, 23:09	0.59 ± 0.03	0.22 ± 0.03		1.64 ± 0.05
1985, 185, 15:48	186, 03:00	0.59 ± 0.04	0.26 ± 0.02		1.68 ± 0.03
1986, 009, 23:50	010, 11:58	2.17 ± 0.07			3.47 ± 0.04
1986, 010, 00:09 ^d	011, 02:11	2.17 ± 0.07			3.06 ± 0.04

^a Format: year, day, hour: minutes.

^b Format: day, hour: minutes.

^c ME count rates are for PHA channels 1 to 35 corresponding to the energy range 1–10 keV with the best signal-to-noise ratio.

^d Detector 3 was off during ME observation.

Table 2. Model 1: power-law + absorption

Date	Γ^a	N^b	N_{H}^c	$\chi^2/\text{d.o.f.}$
1984/154	$1.85^{+0.07}_{-0.07}$	$10.92^{+0.96}_{-0.92}$	$1.04^{+0.32}_{-0.27}$	1.79/27
1984/183	1.76	11.96	1.33	3.45/27
1985/176	1.22	1.73	0.00	2.70/27
1985/180	$1.66^{+0.12}_{-0.11}$	$4.06^{+0.69}_{-0.58}$	$1.09^{+0.64}_{-0.45}$	1.27/27
1985/185	$1.64^{+0.07}_{-0.09}$	$4.06^{+0.43}_{-0.38}$	$1.04^{+0.46}_{-0.34}$	0.98/27
1986/009	$1.98^{+0.05}_{-0.05}$	$13.65^{+0.91}_{-0.83}$	$1.58^{+0.28}_{-0.25}$	1.94/27
1986/010	1.97	11.79	1.29	3.89/27

^a Photon index.

^b Normalization in $10^{-3} \text{ photons cm}^{-2} \text{ s}^{-1} \text{ keV}^{-1}$ at 1 keV.

^c Column density in 10^{20} cm^{-2} .

aligned to the pointing axis or offset by 2° to monitor the background emission. Background subtraction of the ME spectra were carried out using “swap” technique (Smith 1984; White & Peacock 1988; Yaqoob et al. 1989). The log of LE and ME observations with the corresponding count rates are presented in Table 1. X-ray spectral fitting (XSPEC; Shafer et al. 1989) software package was used for the analysis of the LE and ME spectra of NGC 4593 and all the spectra were analysed separately to avoid the systematic effects due to background variations and possible source variations. Detailed spectral analysis procedure has been described in previous papers (Ghosh & Soundararajaperumal 1991a, b).

3. Results and discussion

The best-fitting parameters of model 1 (power-law + absorption) show that the derived N_{H} values are smaller than the galactic N_{H} value ($2.3 \times 10^{20} \text{ cm}^{-2}$) (see Table 2). In model 2 (power-law + fixed absorption) we fix the column

density to the galactic value (see Table 3). Figure 1 shows the plot of the LE + ME spectra (photon spectra) of NGC 4593 with best fit power-law + fixed absorption model convolved through the detector response. The lower panel of this figure shows the residuals between the spectra and the model. The residuals of Fig. 1 show the presence of soft excess emission in this galaxy. However, forcing a column density in the presence of a soft excess always steepens the spectral slope and decreases the soft excess values (Ghosh & Soundararajaperumal 1992a, b and references therein). This type of spectral steepening is also present in NGC 4593 which can be seen from the comparison of the Γ values between models 1 and 2 (see Tables 2 and 3). Thus the true soft excess values may be obtained by measuring the excess flux above the ME power-law extrapolation. Figures 2a and b show the plots of the residuals between the spectra and fixed power-law (obtained from the fits to the ME data only) + fixed absorption model. Two power-law (model 3), thermal bremsstrahlung (model 4) and broken power-law models (model 5) were used to fit the soft excess emissions of the galaxy. Reduced χ^2 values show that the broken power-law model fits better than that obtained from the two power-law and the thermal bremsstrahlung models (see Tables 4–6).

Presence of emission feature around 6 keV can be seen from the residuals of Fig. 1. We used the power-law + fixed absorption + gaussian-line model (model 6) to fit the emission feature and the results are given in Table 7. Figure 3 shows the photon spectra of NGC 4593 fitted with model 6 and the residuals are shown in the lower panel of this figure.

Comparison of the Uhuru and Ariel V fluxes of NGC 4593 suggests that the source has increased in intensity between 1970–73 and 1975 December (Bell Burnell & Culhane 1979). The hard (2–10 keV) X-ray flux of this galaxy was $2.01 \times 10^{-11} \text{ erg cm}^{-2} \text{ s}^{-1}$ when it was ob-

Table 3. Model 2: power-law + fixed absorption^a

Date	Γ^b	N^c	Flux ^d		L_x^e		$\chi^2/\text{d.o.f.}$
			0.1–2 (keV)	2–10 (keV)	0.1–2 (keV)	2–10 (keV)	
1984/154	2.01	13.48	3.88 ± 0.23	3.40 ± 0.05	1.36 ± 0.08	1.19 ± 0.02	2.76/28
1984/183	1.84	13.27	3.66 ± 0.25	4.33 ± 0.05	1.28 ± 0.09	1.52 ± 0.02	3.86/28
1985/176	$1.82^{+0.05}_{-0.04}$	$3.96^{+0.21}_{-0.23}$	1.08 ± 0.07	1.32 ± 0.04	0.38 ± 0.02	0.46 ± 0.01	0.83/28
1985/180	$1.85^{+0.05}_{-0.05}$	$5.20^{+0.28}_{-0.29}$	1.43 ± 0.07	1.68 ± 0.05	0.50 ± 0.02	0.59 ± 0.02	1.50/28
1985/185	$1.77^{+0.05}_{-0.04}$	$4.95^{+0.26}_{-0.26}$	1.35 ± 0.09	1.78 ± 0.03	0.47 ± 0.03	0.62 ± 0.01	1.44/28
1986/009	2.09	15.64	4.62 ± 0.15	3.51 ± 0.04	1.62 ± 0.05	1.23 ± 0.01	2.48/28
1986/010	2.14	14.61	4.39 ± 0.14	3.04 ± 0.04	1.54 ± 0.05	1.06 ± 0.01	4.93/28

^a Fixed at the galactic N_{H} value ($2.3 \cdot 10^{20} \text{ cm}^{-2}$).

^b Photon index.

^c Normalization in $10^{-3} \text{ photons cm}^{-2} \text{ s}^{-1} \text{ keV}^{-1}$ at 1 keV.

^d Flux in $10^{-11} \text{ erg cm}^{-2} \text{ s}^{-1}$.

^e Luminosity in $10^{43} \text{ erg s}^{-1}$.

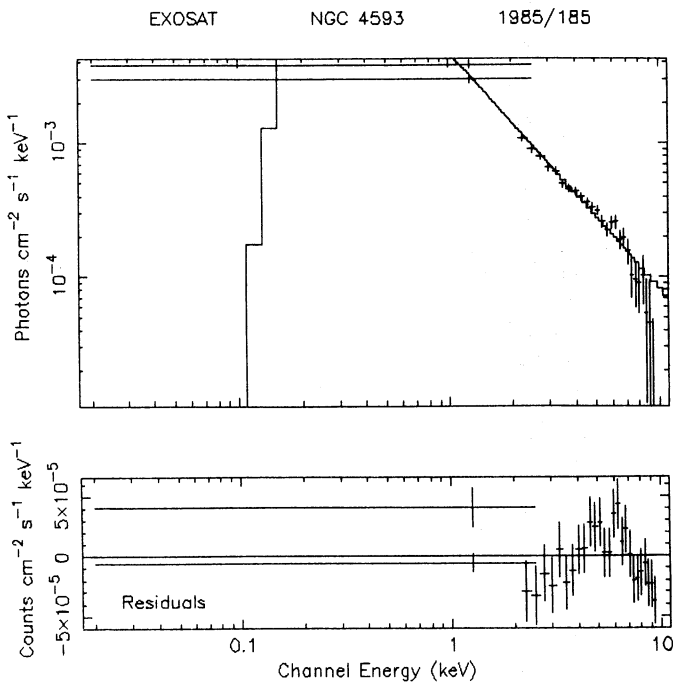


Fig. 1. LE+ME photon spectrum of NGC 4593 for 1985/185 fitted with a power-law + fixed absorption model. Lower panel of the figure shows the residuals between the spectrum and the model

served with Einstein on 1979/176 (Holt et al. 1989) which did not show dramatic variations of this source compared with the previous observations with Uhuru and Ariel V. However this galaxy displayed remarkable intensity variations during EXOSAT observations between 1984 and 1986. In particular the LE count rates show a factor of 5 decrease in a year (between 1984/183 and 1985/176) and a factor 3.7 increase in 189 d (between 1985/185 and 1986/009; see Table 1). In a year interval the ME count rates also decreased, although only by a factor 3 and

increased in 189 d only by a factor 2. Both the LE and ME count rates increased by factors of 1.4 and 1.2, respectively, in 4 d (between 1985/176 and 1985/180) time interval (short time-scale changes of this galaxy have been described by Barr et al. 1987 and Grandi et al. 1992). This differential and uncorrelated (see Fig. 4) variability of the LE and ME count rates on short and long time-scales indicate that the low and medium energy X-ray emissions are from distinct sources.

Spectral index value, $\alpha = (\Gamma - 1)$, of this galaxy measured with Ariel V (Bell Burnell & Culhane 1979) in the 2–10 keV range is somewhat steeper ($\alpha = 1.0$) than that obtained with Einstein SSS+MPC data ($\alpha = 0.12^{+0.28}_{-0.24}$; Holt et al. 1989). However the EXOSAT ME spectral index values range from 0.55 to 1.0 and the average slope is $\langle \alpha \rangle = 0.8 \pm 0.1$. Also we do not find any significant variations of α during the EXOSAT observations. The values of α for the LE+ME fits are steeper than the average ME slope. This is because of the presence of soft excess emission in the spectra of the galaxy. Broken power-law model (soft excess modeled by steep power-law below 0.6 keV) describes significantly better fits to the data, over the energy range 0.1–10 keV, than a single power-law model (for comparison see Tables 3 and 6). The best fit spectral index values of the steep power-law (α_1) fits at low energy (below 0.6 keV) are in the range 1.03–1.97 and no remarkable variations of α_1 were present in this galaxy between 1984 and 1986. The steep power-law slopes (α_1) of NGC 4593 are relatively less steeper than usually found in other Seyfert galaxies (Ghosh & Soundararajaperumal 1992c) in which soft excess emissions are present. These low values of α_1 cannot completely fit the soft excess emissions present in this galaxy and as a result of this we still find the presence of some more soft emissions in the residuals of the broken power-law fits (Figs. 5a, b). These results suggest that, most probably, two soft emission components are present in NGC 4593. However, runs made with broken power-law + black body (or thermal

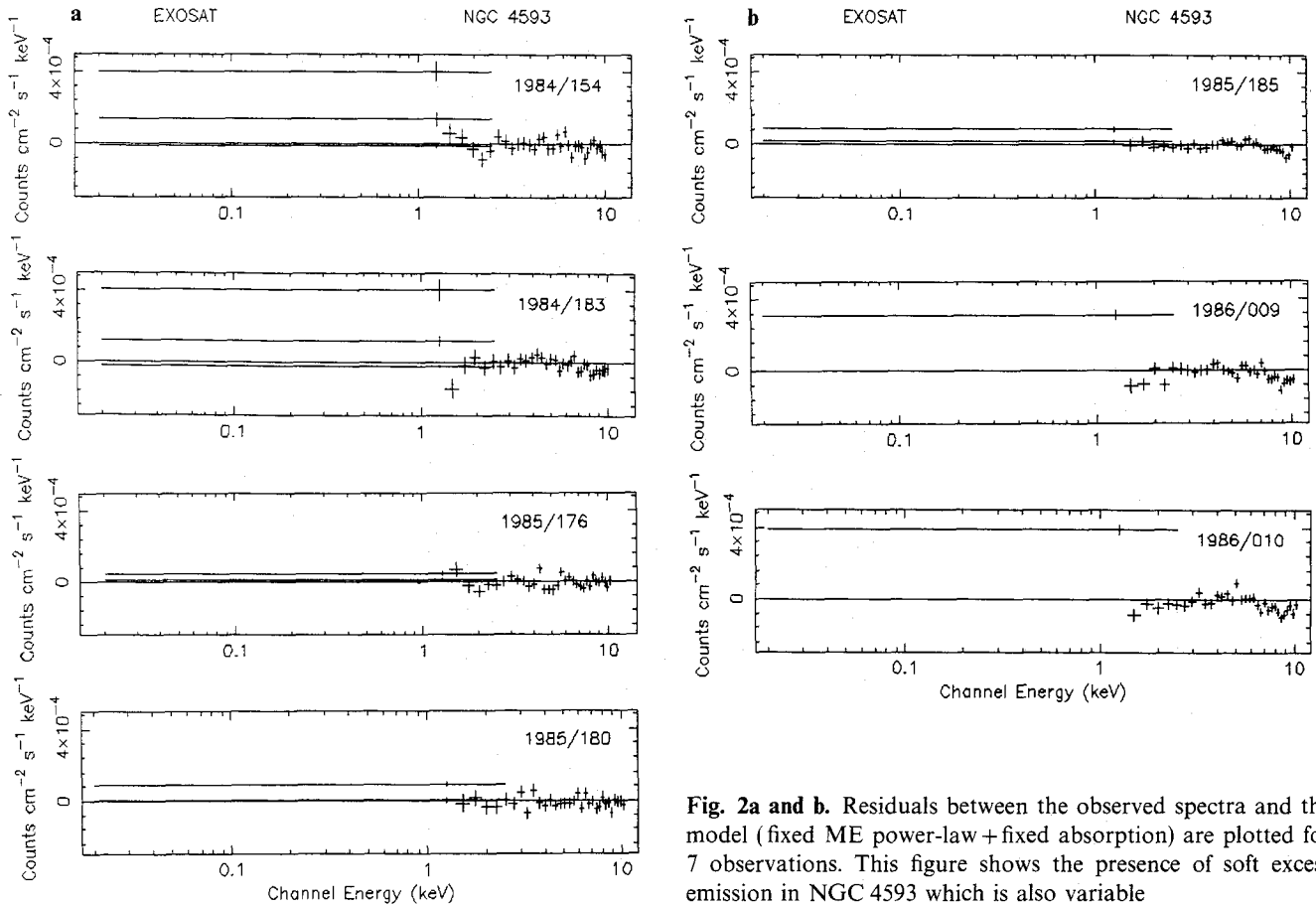


Fig. 2a and b. Residuals between the observed spectra and the model (fixed ME power-law + fixed absorption) are plotted for 7 observations. This figure shows the presence of soft excess emission in NGC 4593 which is also variable

Table 4. Model 3: two power-law + fixed absorption^a

Date	Γ_1^b	N_1^c	Γ_2^b	N_2^c	$\chi^2/\text{d.o.f.}$
1984/154	$3.91^{+1.10}_{-0.90}$	$0.89^{+2.52}_{-0.74}$	$1.80^{+0.08}_{-0.10}$	$10.22^{+1.08}_{-1.75}$	1.45/27
1984/183	4.17	0.59	1.71	11.48	3.00/27
1985/176	$2.11^{+0.54}_{-0.47}$	$1.29^{+0.77}_{-0.61}$	$1.71^{+0.44}_{-0.38}$	$2.58^{+0.31}_{-0.33}$	0.83/27
1985/180	$2.29^{+0.58}_{-0.52}$	$0.77^{+0.52}_{-0.32}$	$1.69^{+0.41}_{-0.40}$	$4.22^{+0.67}_{-0.56}$	1.25/27
1985/185	$2.37^{+0.49}_{-0.44}$	$0.89^{+0.41}_{-0.40}$	$1.64^{+0.33}_{-0.30}$	$4.11^{+0.41}_{-0.39}$	0.96/27
1986/009	$4.68^{+1.03}_{-0.95}$	$0.36^{+0.24}_{-0.19}$	$1.77^{+0.37}_{-0.34}$	$13.70^{+1.54}_{-1.42}$	1.78/27
1986/010	4.94	0.39	1.78	11.90	3.81/27

^a Fixed at the galactic N_{H} value ($2.3 \cdot 10^{20} \text{ cm}^{-2}$).

^b Photon index.

^c Normalization in $10^{-3} \text{ photons cm}^{-2} \text{ s}^{-1} \text{ keV}^{-1}$ at 1 keV.

bremsstrahlung) model do not significantly improve the χ^2_r values than the broken power-law fit. LE and ME count rates though varied in concert (Table 1) but they are not correlated which can be seen from Fig. 4. In fact from this figure it can be seen that during the brighter state of NGC 4593 the ME count rates varied with, almost, constant LE count rates. Again the LE count rates and the corresponding soft excess emissions are correlated and they were maximum with no variations during the brighter state of this galaxy (Fig. 6). Also from Fig. 7 which shows

the plot of the hard power-law slope versus source brightness, it can be seen that the hard power-law slope was almost constant even though the source brightness varied. From Table 2 it can be also seen that the N_{H} values were nearly equal to the Galactic N_{H} value, which suggest that the absorbing columns did not vary with the source brightness. For certain galaxies it was found that their spectra become softer as they get brighter (Grandi et al. 1992 and references therein). However we do not find any such relation in NGC 4593, even though the brightness of this

Table 5. Model 4: thermal bremsstrahlung+fixed absorption^a

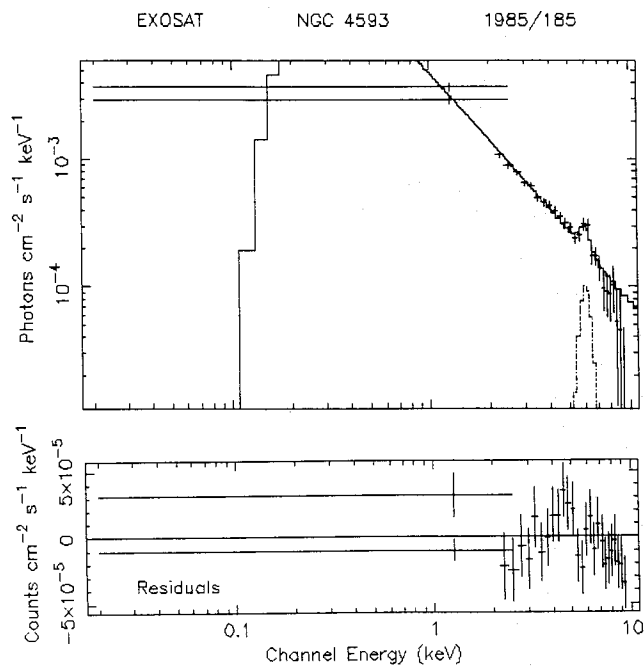
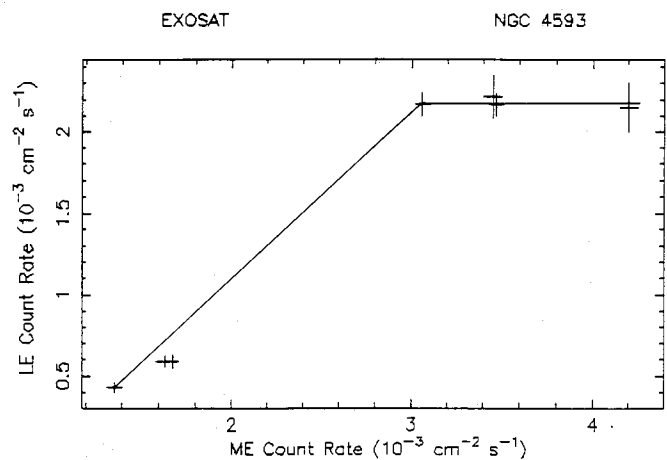
Date	kT ^b	N ^c	χ^2_r /d.o.f.
1984/154	5.64	5.07	8.9/28
1984/183	7.17	5.00	7.0/28
1985/176	3.85	2.86	2.6/28
1985/180	4.29	3.24	4.1/28
1985/185	6.92	2.10	4.7/28
1986/009	4.38	6.95	20.0/28
1986/010	4.40	6.07	22.6/28

^a Fixed at the galactic N_H value ($2.3 \times 10^{20} \text{ cm}^{-2}$).^b Plasma temperature in keV.^c Normalization in $10^{-3} \text{ photons cm}^{-2} \text{ s}^{-1} \text{ keV}^{-1}$ at 1 keV.**Table 6.** Model 5: broken power-law^a+fixed absorption^b

Date	Γ_1^c	Γ_2^c	N ^d	χ^2_r /d.o.f.
1984/154	$2.97^{+0.20}_{-0.22}$	$1.82^{+0.06}_{-0.06}$	$5.86^{+1.39}_{-1.11}$	1.24/27
1984/183	2.77	1.72	6.67	2.70/27
1985/176	$2.04^{+0.47}_{-0.34}$	$1.77^{+0.14}_{-0.13}$	$3.23^{+2.14}_{-1.20}$	0.84/27
1985/180	$2.08^{+0.38}_{-0.42}$	$1.68^{+0.12}_{-0.13}$	$2.74^{+1.48}_{-0.94}$	1.34/27
1985/185	$2.03^{+0.30}_{-0.33}$	$1.62^{+0.08}_{-0.09}$	$2.51^{+0.92}_{-0.65}$	1.01/27
1986/009	$2.78^{+0.15}_{-0.16}$	$1.78^{+0.05}_{-0.05}$	$10.63^{+1.90}_{-1.58}$	1.93/27
1986/010	2.94	1.77	8.12	3.87/27

^a Break energy fixed at 0.6 keV.^b Fixed at the galactic N_H value ($2.3 \times 10^{20} \text{ cm}^{-2}$).^c Photon index.^d Normalization in $10^{-3} \text{ photons cm}^{-2} \text{ s}^{-1} \text{ keV}^{-1}$ at 1 keV.**Table 7.** Model 6: power-law + fixed absorption^a + gaussian line

Date	Γ^b	N ^c	E_L^d	E_N^e	EW ^f	χ^2_r /d.o.f.
1985/185	$1.81^{+0.04}_{-0.05}$	$5.02^{+0.25}_{-0.26}$	$6.04^{+0.49}_{-1.26}$ <td>$0.81^{+0.41}_{-0.40}$</td> <td>380 ± 190</td> <td>1.10/26</td>	$0.81^{+0.41}_{-0.40}$	380 ± 190	1.10/26
1986/009	$2.12^{+0.03}_{-0.02}$	$15.92^{+0.45}_{-0.45}$	$5.08^{+0.30}_{-0.26}$	$0.89^{+0.55}_{-0.55}$	190 ± 95	1.78/26
1986/010	2.17	14.67	5.7	1.58	439	2.64/26

^a Fixed at the galactic N_H value ($2.3 \times 10^{20} \text{ cm}^{-2}$).^b Photon index.^c Normalization in $10^{-3} \text{ photons cm}^{-2} \text{ s}^{-1} \text{ keV}^{-1}$ at 1 keV.^d Line energy in keV.^e Line intensity in $10^{-4} \text{ photons cm}^{-2} \text{ s}^{-1}$.^f Equivalent width in eV.**Fig. 3.** Photon spectrum of NGC 4593 for 1985/185 fitted with the power-law + fixed absorption + Gaussian line model (model 6). Lower panel of the figure shows the residuals between the spectrum and the model**Fig. 4.** Plot of the LE versus ME count rates. Note that they are not correlated

galaxy varied dramatically during EXOSAT observations (see Fig. 7). This type of complex variation of soft excess emission and the LE and ME count rates can be understood if we know their origin.

We have computed the value of “ g ” using the expression given in Elvis et al. (1991) and we suggest (based on

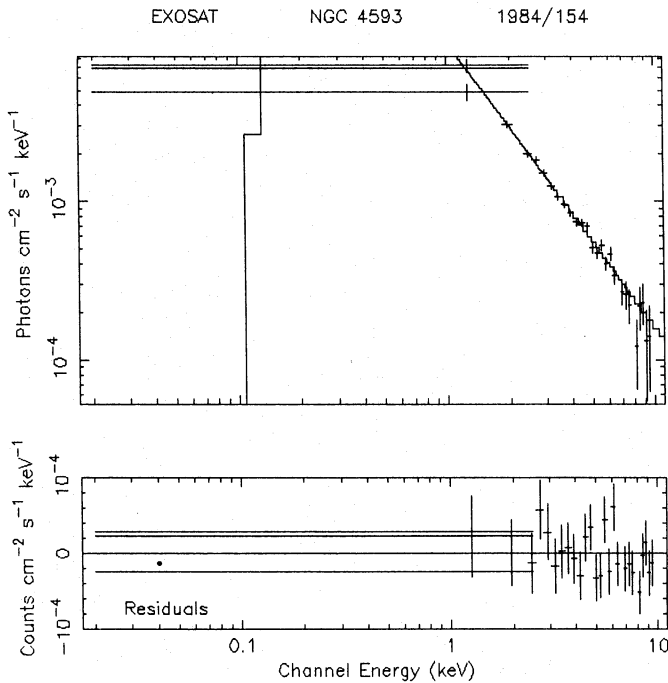


Fig. 5a. LE + ME photon spectrum of NGC 4593 for 1984/154 fitted with the broken power-law model. The residuals between the spectrum and the model are shown in the lower panel of this figure. Still the presence of soft excess emission can be seen from the residuals

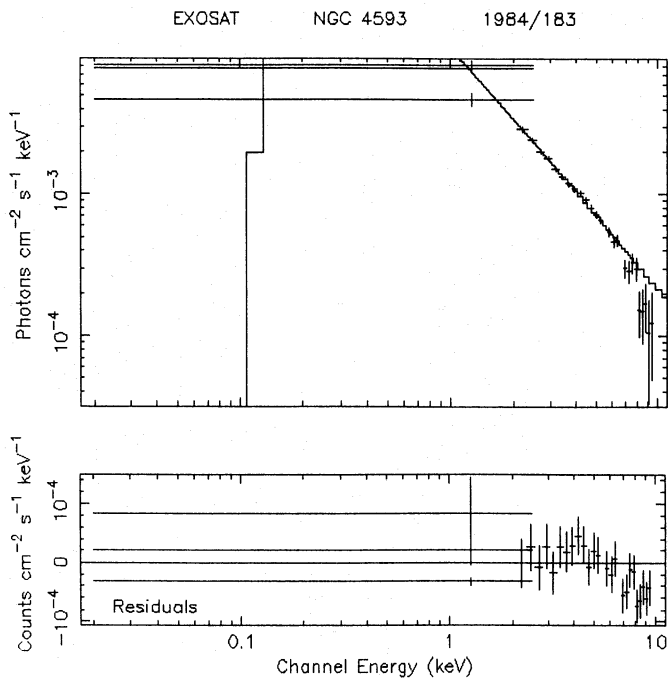


Fig. 5b. Same as Fig. 5a but for 1984/183

the obtained value of “ g ”) that the soft excess emissions detected in this galaxy, may be, due to optically thick emission from the inner regions of an accretion disk, which was already suggested by Elvis et al. (1991) for other

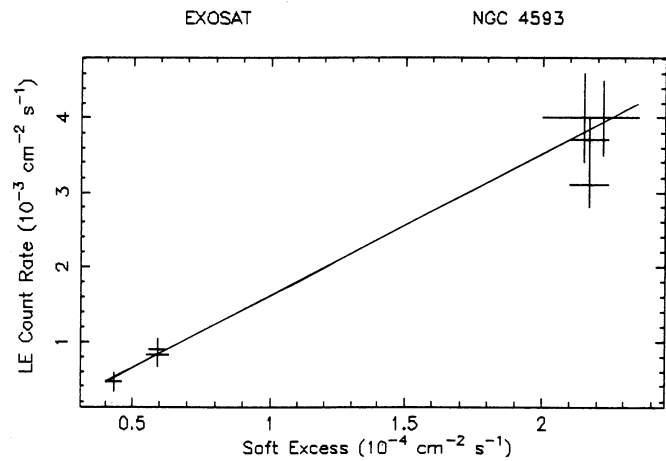


Fig. 6. Measured soft excess values are plotted against the observed LE count rates. Solid line shows that these two parameters are correlated

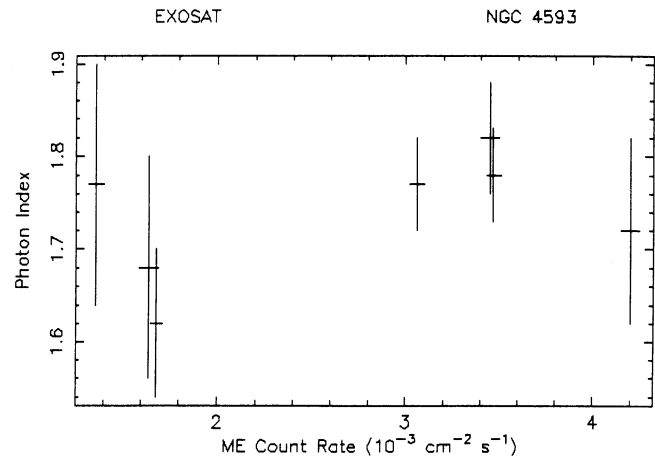


Fig. 7. Plot of the hard spectral slopes versus ME count rates

AGNs. However, we are not sure about the presence of the probable second soft emission component and if it is present, then most probably it is due to thermal emission with electron scattering. Since we exactly do not know the origin of different X-ray emissions, so at present it is difficult to make comments about the complex variations of the LE and ME count rates and soft excess emissions of NGC 4593.

From the results of the spectral analysis we find that there are signatures for the presence of an emission line around 6.0 keV in the spectra of NGC 4593 (see Fig. 2a, b). We find a significant improvement in the fit (see Tables 3 and 7 to compare the χ_r^2 values) using the Gaussian line model (model 6) over the simple power-law model (model 2). It is interesting to note that the values of the spectral slopes are steeper with the Gaussian model (model 6) than that obtained from the simple power-law model (model 2). This type of spectral steepening has been also found in the spectra of Seyfert galaxies observed with GINGA

Table 8. Model 7: broken power-law + fixed absorption^a + gaussian line

Date	Γ_1^b	Γ_2^b	N^c	E_L^d	E_N^e	EW ^f	$\chi_r^2/\text{d.o.f.}$
1985/185	$2.35^{+0.4}_{-0.3}$	$1.69^{+0.10}_{-0.12}$	$3.07^{+1.4}_{-0.92}$	$6.0^{+0.5}_{-1.2}$	$0.59^{+0.40}_{-0.39}$	276 ± 175	0.91/25
1986/009	$2.91^{+0.24}_{-0.24}$	$1.85^{+0.08}_{-0.08}$	$12.90^{+3.8}_{-2.8}$	$5.1^{+0.32}_{-0.60}$	$0.56^{+0.38}_{-0.35}$	105 ± 68	1.43/25
1986/010	3.09	1.90	9.46	5.6	0.94	242	2.27/25

^a Fixed at the galactic N_H value ($2.3 \times 10^{20} \text{ cm}^{-2}$).

^b Photon index.

^c Normalization in $10^{-3} \text{ photons cm}^{-2} \text{ s}^{-1} \text{ keV}^{-1}$ at 1 keV.

^d Line energy in keV.

^e Line intensity in $10^{-4} \text{ photons cm}^{-2} \text{ s}^{-1}$.

^f Equivalent width in eV.

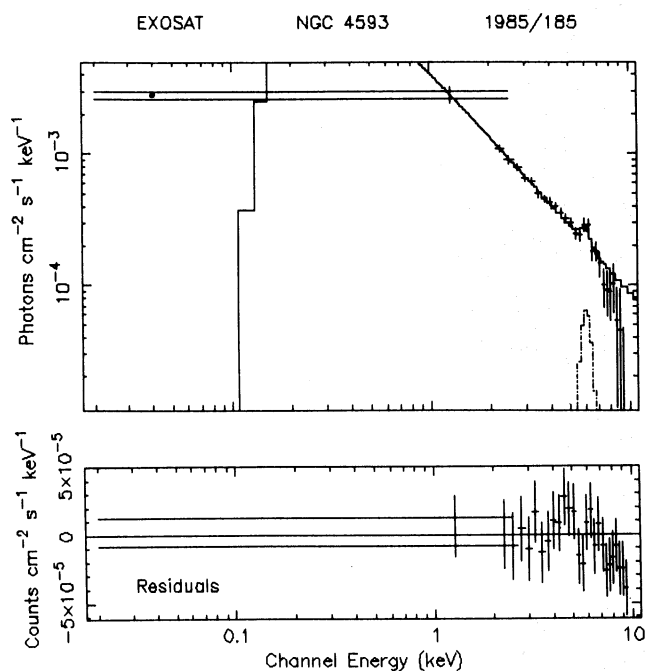


Fig. 8. Photon spectrum of NGC 4593 for 1985/185 fitted with the broken power-law + fixed absorption + Gaussian line model (model 7). Lower panel of the figure shows the residuals between the spectrum and the model

(Matsuoka et al. 1990; Pounds et al. 1990). Also the presence of an iron line at 6.4 keV with equivalent width around 150 ± 20 eV, was detected in several Seyfert galaxies (Matsuoka et al. 1990; Piro et al. 1990; Pounds et al. 1990). It has been suggested that the iron line is produced due to the reprocessing of the intrinsic emission by a cold and optically thick medium due to fluorescence (Pounds et al. 1990; Matsuoka et al. 1990). Also it has been found that both the equivalent width and the relative intensity of the reflected component to the direct emission agree well with the expected values obtained from an accretion disk with solar-like abundances seen face-on (Matt et al. 1991). Due to the non-availability of the “reflection model” in the XSPEC software package, we are unable to fit the X-ray

spectra of NGC 4593 with this model. However the best-fitting parameters of the Gaussian line model (model 6) suggest that the reprocessing of the central continuum emission by a thick cold matter produces the detected emission line, around 6.0 keV, by fluorescence of iron.

Broken power-law + photoelectric absorption (fixed with the Galactic N_H value) + a Gaussian-line model (model 7) was used to fit the spectra and the best-fitting parameters are given in Table 8. Figure 8 shows the photon spectra of NGC 4593 fitted with model 7 and the residuals are shown in the lower panel of this figure. These results suggest that the X-ray spectrum of NGC 4593 consists of three components: a variable soft spectral component below 0.6 keV, a nonvariable hard spectral component above 0.6 keV (0.6–10 keV), and a fluorescent iron emission line around 6.0 keV which is produced due to the reprocessing of the intrinsic emission by a thick cold matter around the central continuum source.

Acknowledgements. We are grateful to Prof. J.C. Bhattacharyya for his support and encouragement, in all respects. Our thanks to the EXOSAT Observatory staff, especially to Drs. N.E. White, A.N. Parmar, F. Habrel, P. Giommi, P. Barr and A.M.T. Pollock, at ESTEC who helped us to get the data from the archives and provided us with the XSPEC software package. One of us, KKG, wants to express his sincere thanks to the EXOSAT staff for their help in data analysis during his stay at ESTEC. Our sincere thanks to Dr. K.A. Pounds for valuable comments and suggestions.

References

- Barr P., Clavel J., Giommi P., Mushotzky R.F., Madejski G., 1987, in: Treves (ed.) Proc. Villa Olmo Meeting. AADA, Milano, p. 43
- Bell Burnell S.J., Culhane J.L., 1979, MNRAS 188, 1P
- de Korte P.A.J., Bleeker J.A.M., den Boggende A.J.F., Branduardi-Raymont G., Culhane J.L., Gronenschild E.H.B.M., Mason I., McKechnie S.P., 1981, Space Sci. Rev. 30, 495
- Elvis M., Giommi P., Wilkes B.J., McDowell J., 1991, ApJ 378, 537
- Forman W., Jones C., Cominsky L., Julien P., Murray S., Peters G., Tananbaum H., Gioconci R., 1978, ApJS 38, 357

- Ghosh K.K., Soundararajaperumal S., 1991a, AJ 102, 1298
Ghosh K.K., Soundararajaperumal S., 1991b, ApJ 383, 574
Ghosh K.K., Soundararajaperumal S., 1992a, ApJ 389, 179
Ghosh K.K., Soundararajaperumal S., 1992b, PASP 104, 258
Ghosh K.K., Soundararajaperumal S., 1992c, MNRAS 254, 563
Grandi P., Tagliaferri G., Giommi P., Barr P., Palumbo G.G.C., 1992, ApJS (in press)
Hayes M.J.C., Bell Burnell S.J., Culhane J.L., Ward M.J., Barr P., Ives J.C., Sanford P.W., 1981, Space Sci. Rev. 30, 39
Holt S.S., Turner T.J., Mushotzky R.F., Weaver K., 1989, in: Hunt J., Battick B. (eds.) Proc. 23rd ESLAB Symp. on Two Topics in X-ray Astronomy (ESA SP-296). Noordwijk, ESA, p. 1105
MacAlpine G.M., Williams G.A., Lewis D.W., 1979, PASP 91, 746
Marshall F.E., Mushotzky R.F., Boldt E.A., Holt S.S., Rothschild R.E., Serlemitsos P.J., 1978, Nat 275, 624
Matsuoka M., Piro L., Yamauchi M., Murakami T., 1990, ApJ 361, 440
Matt G., Perola G.C., Piro L., 1991, A&A 247, 25
Mitchell R.J., Dickens R.J., Bell Burnell S.J., Culhane J.L., 1979, MNRAS 189, 329
Piro L., Yamauchi M., Matsuoka M., 1990, ApJ 360, L35
Pounds K.A., Nandra K., Stewart G.C., George I.M., Fabian A.C., 1990, Nat 344, 132
Simkin S.M., Su H.J., Schwarz M.P. 1980, ApJ 237, 404
Smith A., 1984, EXOSAT Express No. 5, 48
Turner M.J.L.T., Smith A., Zimmermann H.U., 1981, Space Sci. Rev. 30, 513
Turner T.J., Pounds K.A., 1989, MNRAS 240, 833
Ulvestad J.S., Wilson A.S., 1984, ApJ 285, 439
Veron-Cetty M.P., Veron P., 1986, A&AS 66, 335
Veron-Cetty M.P., Veron P., Tarengi M., 1982, A&A 113, 46
White N.E., Giommi P., 1991, in: Egret D., Albrecht M. (eds.) Database and On-Line Data in Astronomy (in press)
White N.E., Peacock A., 1988, Mem. Soc. Astron. Ital. 59, 7
Wood K.S., Meekins J.F., Yentis D.J., Smarthers H.W., McNutt D.P., Bleach R.D., Byram E.T., Chubb T.A., Friedman H., 1984, ApJS 56, 507
Yaqoob T., Warwick R.S., Pounds K.A., 1989, MNRAS 236, 153